Supporting Information for

Toward Intrinsic Ultra-High Temperature Ferromagnetism in $CrAuTe_2$/graphene heterosystem

Chaobin Jia, [a,#] *Chao Jin* [b,#] *Puyuan Shi,*[a] *Jingjuan Su,*[a] *Yungeng Zhang,* [a*] *Xianghong Niu,*[b*] *and Bing Wang,* [a*]

[a]Joint Center for Theoretical Physics (JCTP), Institute for Computational Materials Science, School of Physics and Electronics, Henan University, Kaifeng 475004, People's Republic of China.

† These authors have contributed equally to this work

∗ Corresponding Author: 20130016@vip.henu.edu.cn; xhniu@njupt.edu.cn; wb@henu.edu.cn

1. The POSCAR of the monolayer $CrAuTe_2$

monolayer $CrAuTe_2$
1.00000000000000
4.3280418580187732 -0.0000208995614012 0.0000000000000000
-2.1640390285604876 3.7481837478530737 0.0000000000000000
0.0000000000000000 0.0000000000000000 25.0825004577999984
Cr Te Au
1 2 1
Direct
0.0000021381709846 -0.0000021381709846 0.4676178394001452
0.0000005763566264 -0.0000005763566264 0.5785949828986056
0.6666688903105877 0.3333311386894113 0.4207994440774365
0.6666684431617980 0.3333315858382008 0.5329877026238137

2. Two typical magnetic orders

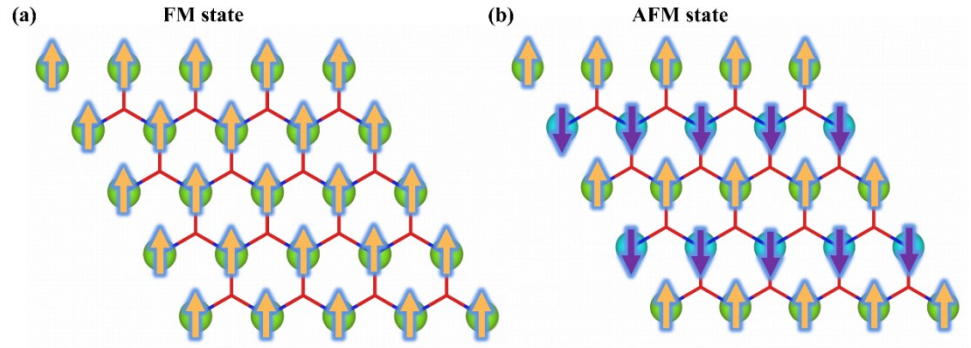

Figure S1 The different magnetic sequencing configurations of monolayer $CrAuTe_2$ from top view. (a) ferromagnetism, (b) antiferromagnetism, where yellow and violet indicate net spin-up spin downward polarization. The rotation up and rotation down directions are indicated by a yellow up arrow and a purple down arrow, indicated by the arrow of the Cr atom.

3. Orientation-dependent Young's modulus and Poisson's ratio

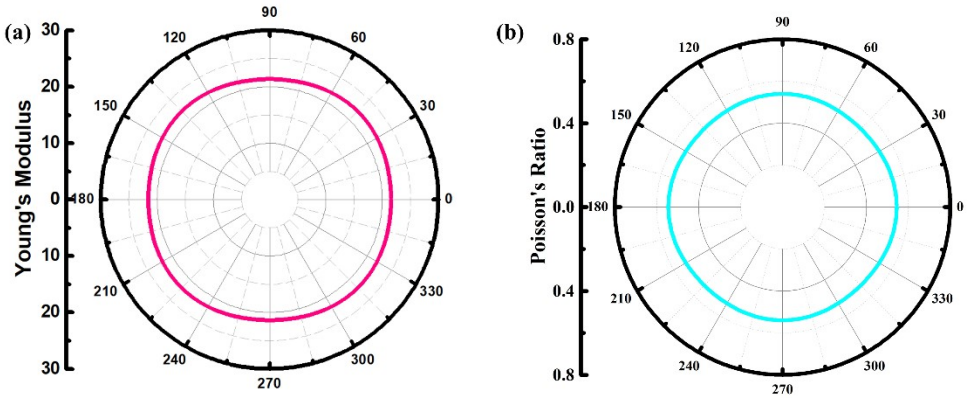

Figure S2 Young's modulus (a) and Poisson's ratio (b) in all directions of the monolayer $CrAuTe_2$ in the x-y plane.

4. Magnetic moment as functions of temperature for 2D FM $CrCl_3$, $CrBr_3$, and CrI_3.

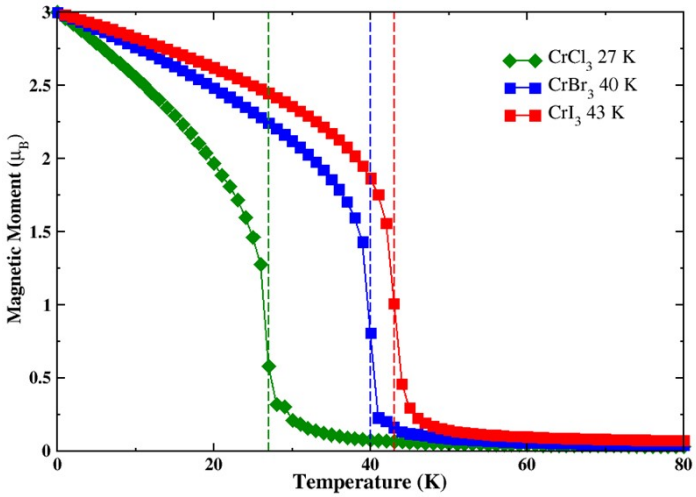

Figure S3. The calculated magnetic moment as functions of temperature for monolayer $CrCl_3$, $CrBr_3$, and CrI_3, respectively.

The calculated T_{Cs} of monolayer $CrCl_3$, $CrBr_3$, and CrI_3 are around 27 K, 40 K, and 43 K (Figure S3), respectively, which are in good agreement with the experimental values of 17 K, [1] 34 K,[2] and 45 K,[3] respectively.

5. The angular dependence of MAE for monolayer $CrAuTe_2$

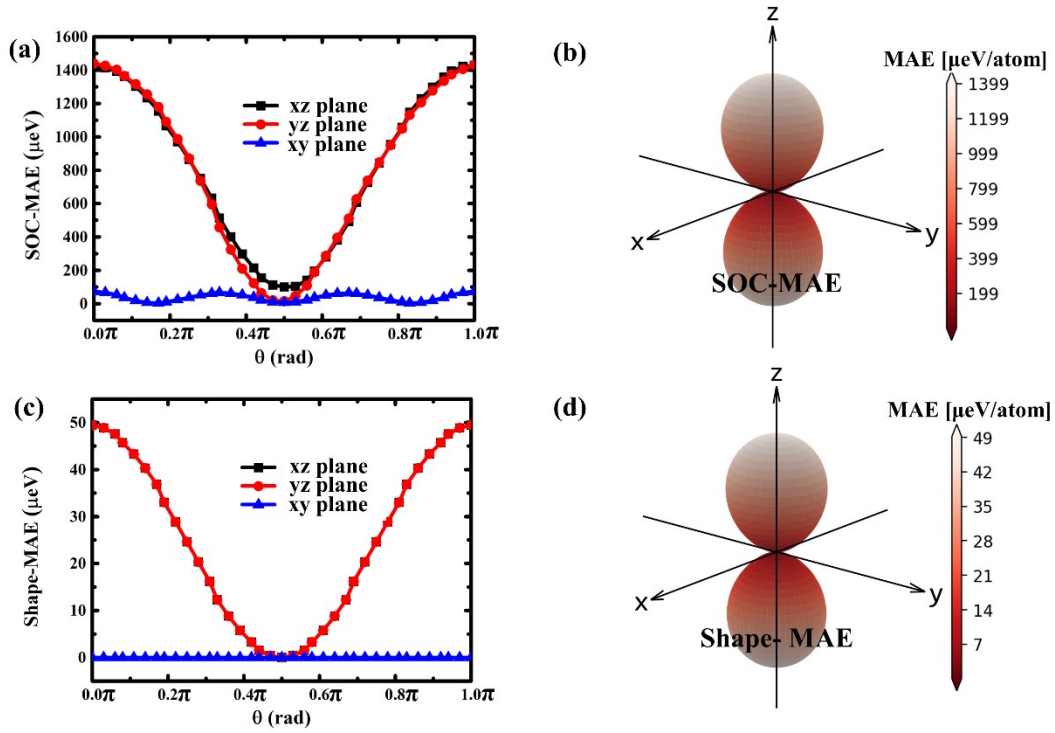

Figure S4. Angular dependence of the MAE of monolayer $CrAuTe_2$ with the direction of magnetization lying on three different planes (xz, yz, and xy planes) (a, c) and the whole space (b, d). The MAE under SOC interaction (a, b) and magnetic dipole-dipole interaction (c, d)

6. The band structures of monolayer $CrAuTe_2$ under strains

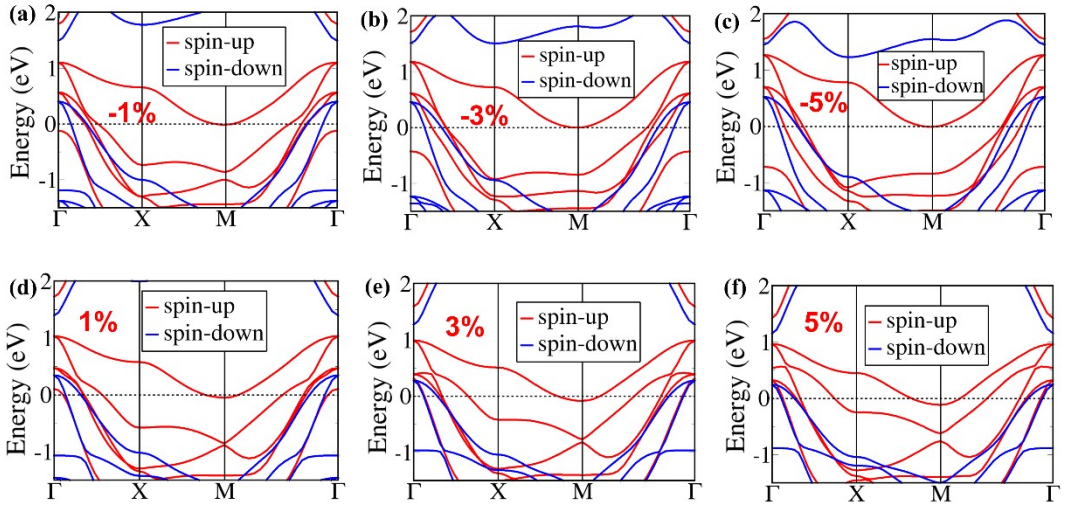

Figure S5 (a ~ f) Band structures of monolayer $CrAuTe_2$ under biaxial strains (-5 %~5%).

7. **Band structures of monolayer $CrAuTe_2$ under electron doping.**

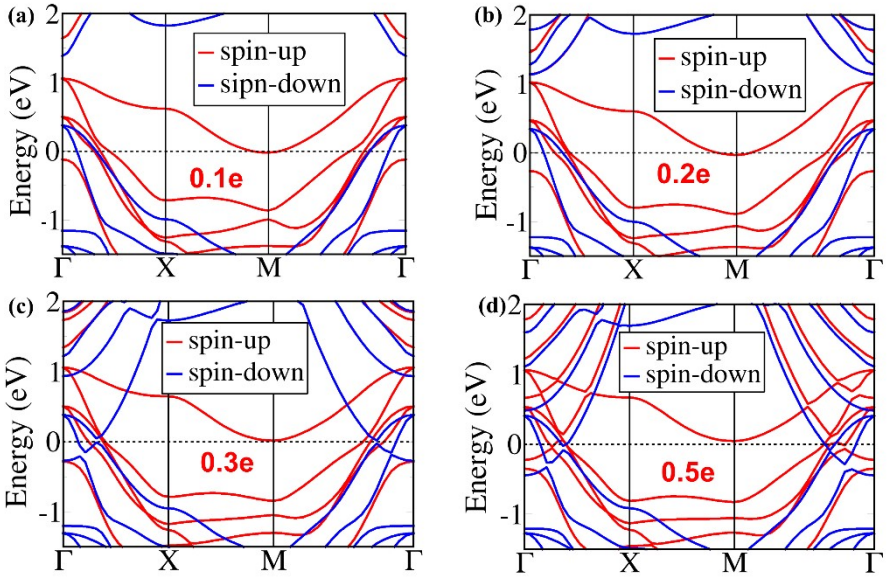

Figure S6 (a ~ d) Band structures of monolayer $CrAuTe_2$ doped with 0.1e, 0.2e, 0.3e, 0.5e.

8. The influence of graphene substrate on the magnetic and electronic properties of $CrAuTe_2$.

Table S1. Energy of primary cell and magnetic moment of Cr ion under four stacking modes.

	Type1	Type2	Type3	Type4	Monolayer
Energy (eV)	-74.882	-74.887	-74.877	-74.874	-
Moment (μ_B)	3.407	3.401	3.398	3.394	3.378

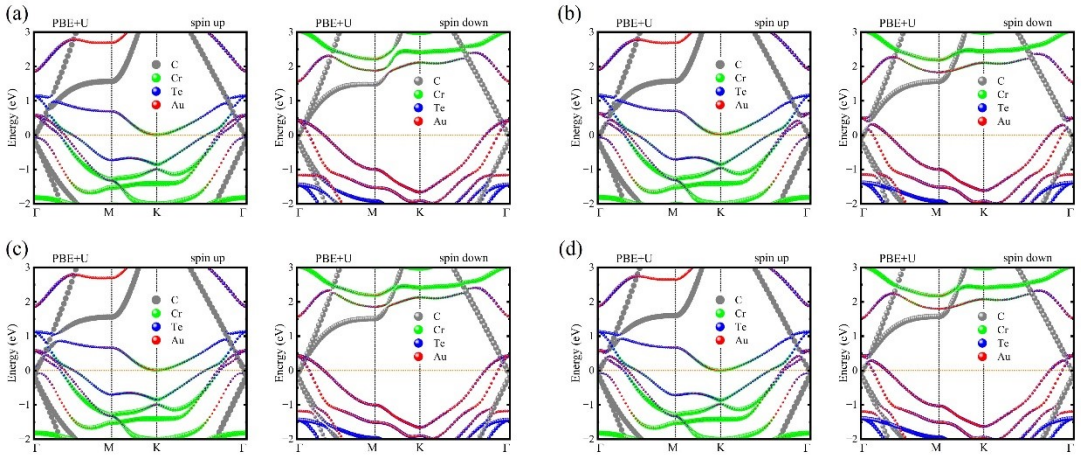

Figure S7 Band structures of $CrAuTe_2$/graphene heterostructure. (a) Type 1 configuration, (b) Type 2 configuration, (c) Type 3 configuration, (d) Type 4 configuration.

1. X. Cai, T. Song, N. P. Wilson, G. Clark, M. He, X. Zhang, T. Taniguchi, K. Watanabe, W. Yao, D. Xiao, M. A. McGuire, D. H. Cobden and X. Xu, *Nano Lett.*, 2019, **19**, 3993-3998.
2. Z. S. Zhang, J. Jiang, C. Rasmita, A. Gao, W. Yu, T., *Nano Lett.*, 2019, **19**, 3138-3142.
3. B. Huang, G. Clark, E. Navarro-Moratalla, D. R. Klein, R. Cheng, K. L. Seyler, D. Zhong, E. Schmidgall, M. A. McGuire, D. H. Cobden, W. Yao, D. Xiao, P. Jarillo-Herrero and X. Xu, *Nature*, 2017, **546**, 270-273.